

# Effect of pressure on the microstructure of an austenitic stainless steel shock-loaded by very short laser pulses

M. GERLAND

*Laboratoire de Mécanique et Physique des Matériaux, URA CNRS 863, B.P. 109–86960 Futuroscope Cedex, France.*

M. HALLOUIN

*Laboratoire d'Énergétique et Détonique, URA CNRS 193, B.P. 109–86960 Futuroscope Cedex, France.*

Irradiation of metallic targets by a high-energy pulsed laser can generate in materials shock waves with pressure amplitudes of the same order as with conventional shocks from explosives, flyer plate impact etc., but with much shorter pulse durations. Experiments were performed with a 0.6 ns pulsed laser on 304 austenitic stainless steel samples. The effects of induced pressure on the microstructure were investigated by transmission electron microscopy in addition to microhardness measurements and are compared with the conventional results. The twin density and the presence of  $\alpha$ -phase are particularly studied. In spite of the very short pulses, twins were present in the observed areas whatever the pressure, while  $\alpha$ -phase embryos were only present in the pressure range 15–25 GPa.

## 1. Introduction

Numerous studies of residual microstructure induced by shock waves in austenitic stainless steels have been performed for a long time [1–3]. These studies have shown that the most important parameters are pressure, stacking-fault energy and pulse duration [4]. In conventional shock, with a pulse duration of about several microseconds, twinning thresholds were found; Murr [4] gives a critical twinning pressure of 12 GPa for a 2  $\mu$ s pulse duration for a 304 stainless steel; Champion and Rohde [5] observed numerous twins in a stainless steel submitted to shock waves at 10 GPa and 2  $\mu$ s pulse duration, while no twinning was present at 65 ns. Laser-generated shock waves have pulse durations much shorter than conventional shocks; they can reach a duration of less than 1 ns for pressure in the range of 5 GPa to several hundreds of GPa. Previous work [6, 7] has shown that residual microstructure induced by laser shock waves is very similar to that observed in conventional shocked materials. In these studies twinning was still present at 10 GPa and 0.6 ns pulse duration. In this paper we present a detailed study of the residual microstructure of a 304 stainless steel irradiated by a pulsed laser of 0.6 ns pulse duration.

## 2. Experimental procedure

The material studied consisted of polycrystalline foils of type 304 stainless steel (wt % 69.86 Fe, 18.73 Cr, 8.80 Ni, 1.62 Mn, 0.49 Si, 0.17 Cu, 0.14 Mo, 0.065 C,

0.029 P, 0.028 S) with an average grain size of 25  $\mu$ m; several investigators [1–3] have studied this material after shock loading and a lot of microstructural results are available in the literature. Before laser irradiation the sample surfaces were mechanically polished up to 3  $\mu$ m by diamond spray, then electrolytically polished with a 90% acetic acid and 10% perchloric acid solution and then covered by a thin layer of black paint to avoid a high temperature rise due to plasma formation.

The experiments were performed using the LULI (Laboratoire pour l'Utilisation des Lasers Intenses, Ecole Polytechnique, Palaiseau, France) neodymium-glass laser. The samples were submitted to laser plane irradiations in the intensity range  $2 \times 10^{11}$  to  $2 \times 10^{12}$  W cm<sup>-2</sup>, with a pulse duration at half maximum of 0.6 ns and with a focal spot of 3 to 6 mm.

Laser-shocked samples were investigated by optical microscopy, Vickers microhardness and transmission electron microscopy (TEM).

Microhardness measurements were made on irradiated surface samples and at different depths; a 25 g load was used for all indentations.

TEM observations were made with a Jeol 100B microscope operating at 100 kV equipped with a double-tilt stage. The final thin foils were obtained using the double-jet technique with a 95% acetic acid and 5% perchloric acid solution operating at 70 V and at 15 °C. Several thin foils were polished on only one side during a part of the thinning process in order to obtain different observation depths.

### 3. Results

The peak ablation pressure corresponding to our experimental conditions was estimated by averaging the results of a scaling law [8] and of extrapolated experimental values [9]. The laser-driven shock wave has a rapid decay by hydrodynamic attenuation; the pressure corresponding to different depths in the sample was evaluated using the SHYLAC code developed in our laboratory [10]. Experimental conditions and maximum pressures are recorded in Table I.

#### 3.1. Microhardness measurements

Impacted surface microhardness evolution with laser incident flux and maximum pressure is illustrated in Fig. 1. The impacted surface microhardness is not very sensitive to incident flux in the range of  $0.5 \times 10^{12}$  to  $1.5 \times 10^{12} \text{ W cm}^{-2}$  (25 to 55 GPa) since it remains in the order of  $400 \text{ kg mm}^{-2}$  (the initial microhardness is  $190 \text{ kg mm}^{-2}$ ). Below  $0.5 \times 10^{12} \text{ W cm}^{-2}$  ( $P < 25 \text{ GPa}$ ) and above  $1.5 \times 10^{12} \text{ W cm}^{-2}$  ( $P > 55 \text{ GPa}$ ) the microhardness decreases rapidly.

Murr and Rose [1] describe a similar evolution of microhardness with maximum pressure in the case of conventional shock-loaded 304 stainless steel. The saturation pressure of 25 GPa, where the microhardness begins to remain nearly constant, is however lower than for conventional shock-loaded materials while the threshold pressure which produces hardening is rather similar, 8–10 GPa. The microhardness value depends on mass loading, and an evolution law with mass loading [11] transforms microhardness values for a 25 g load to values for the 200 g load commonly used in the literature. In this way the peak value of microhardness for laser-shocked materials,  $380 \text{ kg mm}^{-2}$  (25 g load), becomes  $320 \text{ kg mm}^{-2}$  for a 200 g load. This value is lower than that of the peak value of microhardness for conventional shock-loaded materials (200 g load) [1].

These results are confirmed by measurements on a cross-section of the sample. Several indentations were performed on the cross-section for a constant depth, and the mean diameter of all the indentations gave the microhardness value for this depth.

Pressure evolution with depth was calculated with the SHYLAC code. Fig. 2 gives microhardness evolution with pressure for two peak pressure values. In spite of the scatter we can say that hardening appears around 10 GPa and nearly reaches its maximum at 25 GPa.

#### 3.2. TEM observations

Test No. 3 was characterized by an energy of 67 J, corresponding to a surface peak pressure of 45 GPa. At the observation depth of  $55 \mu\text{m}$  the estimated pressure is about 15 GPa. In this case the microstructure is composed of numerous twins as seen in Fig. 3, where two families of twins are visible as well as  $\alpha$  embryos located at the twin intersections. A quantitative study was performed by counting the number of twin sets in each grain and it emerges that 5% of the observed areas are occupied by only one twin set, 45%

TABLE I Experimental conditions

No.	Laser energy (J)	Focal spot (mm)	Incident flux ( $10^{12} \text{ W cm}^{-2}$ )	Peak pressure (GPa)
1	70	3	1.62	60
2	74	3.5	1.28	50
3	67	3.5	1.17	45
4	45	3.5	0.78	35
5	35	3.5	0.60	30
6	72	5.5	0.50	25
7	23	3.5	0.40	20
8	35	5.5	0.25	15

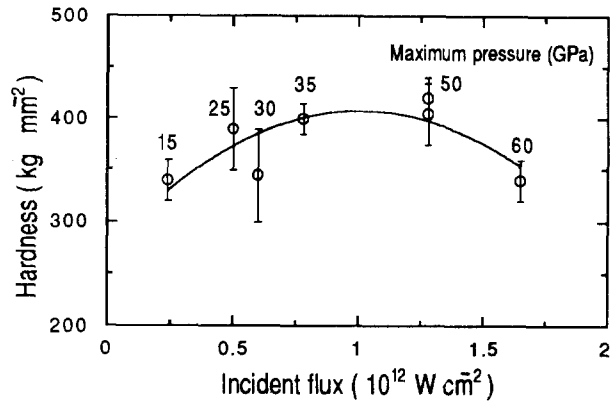


Figure 1 Impacted microhardness evolution with laser incident flux.

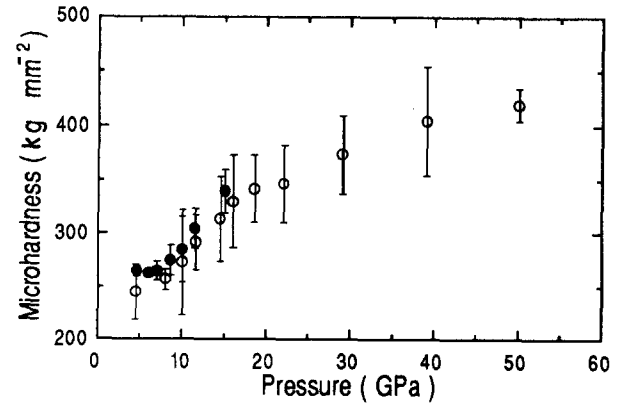


Figure 2 Cross-section microhardness evolution with calculated pressure for two peak pressures: (○)  $P_{\text{max}} = 50 \text{ GPa}$  (test No. 2), (●)  $P_{\text{max}} = 15 \text{ GPa}$  (test No. 8). Pulse duration 0.6 ns.

are occupied by two twin sets and 50% are covered by three or four twin sets. These results are reported in Fig. 4. We have also estimated the mean spacing between twins and the mean thickness of twins in each family, which allows us to calculate the percentage of twinned matter in the shocked material. However, the measured percentage of twinned matter is overestimated for two reasons: first, twins are not always continuous in the whole grain and are sometimes fragmented with untwinned spaces and secondly, when two or several twin families are present in the same grain, the twin intersections are counted two or more times which leads to a not inconsiderable amount. In this foil, the percentage of twinned matter is estimated to

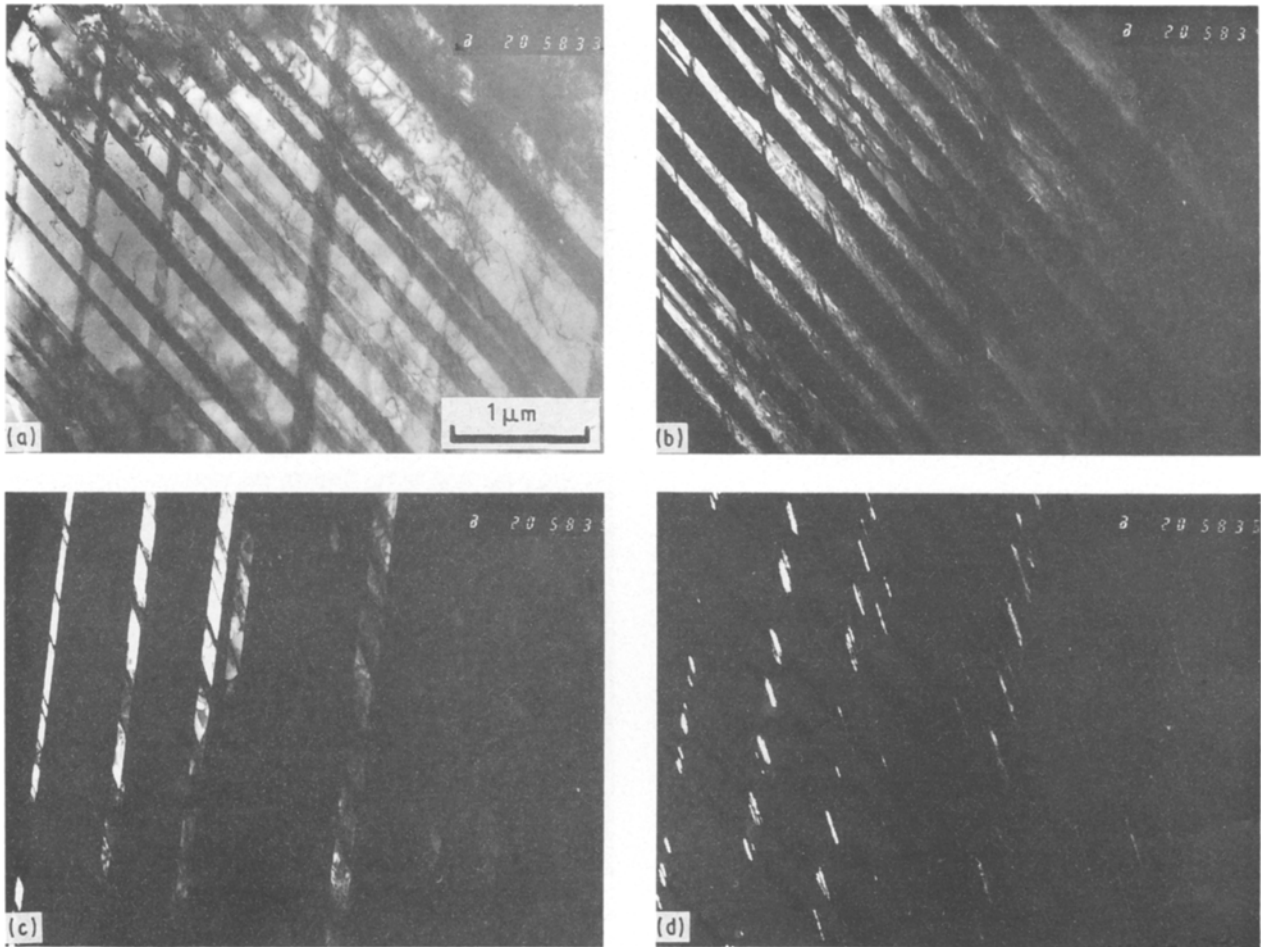


Figure 3 Transmission electron micrographs of sample 3 at a depth of 55  $\mu\text{m}$  corresponding to a 15 GPa shock pressure: (a) bright field showing two sets of twins in a  $(1\ 1\ 2)_\gamma$  section, (b) dark field showing one set of twins, (c) dark field showing a second set of twins, (d) dark field showing  $\alpha$  embryos at the intersections of twin sets.

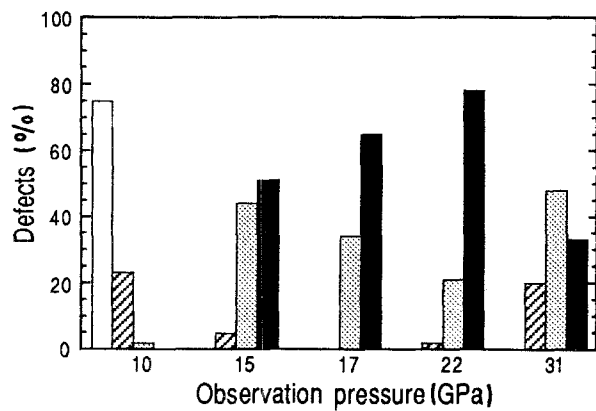


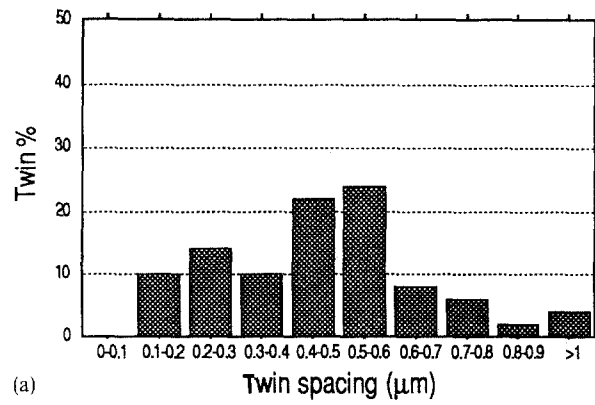
Figure 4 Microstructural evolution with calculated pressure at the observation depth: (□) = only dislocations, (⊗) = 1 twin system, (⊞) = 2 twin systems, (■) = 3 or 4 twin systems.

be 45%. The twin spacings of the different sets with their respective proportions are reported in Fig. 5, where it appears that the mean twin spacing can be estimated as about 0.49  $\mu\text{m}$ .  $\alpha$  embryos were seen in 50% of the grains.

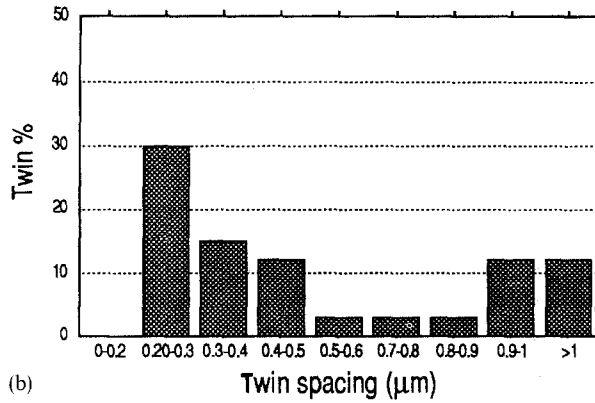
The second sample studied (test No. 5) was characterized by a laser energy of 35 J, corresponding to a surface peak pressure of 30 GPa. However, as the observation depth was situated at only 20  $\mu\text{m}$ , the

estimated pressure at this level was slightly higher than in the previous foil: 17 GPa against 15 GPa. So the microstructure is not very different in the two cases, as seen in Fig. 6 compared to Fig. 3. In this foil, 35% of the observed areas are occupied by two twin sets and 65% by three or four twin sets (Fig. 4). The twin spacings of the different families with their respective proportions are reported in Fig. 5. In this case the mean twin spacing of the whole sample can be estimated about 0.63  $\mu\text{m}$ , and the percentage of twinned matter is about 42%. The higher mean value of twin spacing is due to the presence of several grains with a low twin density.  $\alpha$  embryos were seen in 30% of the observed grains.

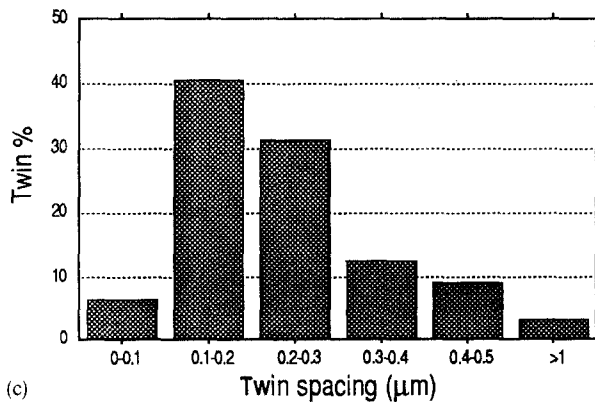
The third sample (test No. 4) was characterized by a laser energy of 45 J corresponding to a surface peak pressure of 35 GPa. As the observation depth was situated at 25  $\mu\text{m}$  below the surface, the estimated pressure at this depth was 22 GPa. Since the pressure is higher in this foil than in the two previous ones, the twin density is higher as seen firstly in Fig. 7, secondly in Fig. 4 where it can be seen that 78% of the observed areas are occupied by three or four twin sets and only 20% are covered by two twin sets, and thirdly in Fig. 5 where the mean twin spacing of the whole sample can be estimated as about 0.33  $\mu\text{m}$ . The percentage of twinned matter is of course higher than in the two



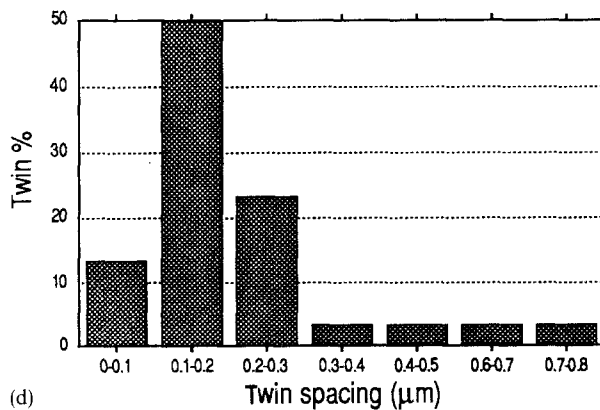
(a)



(b)



(c)

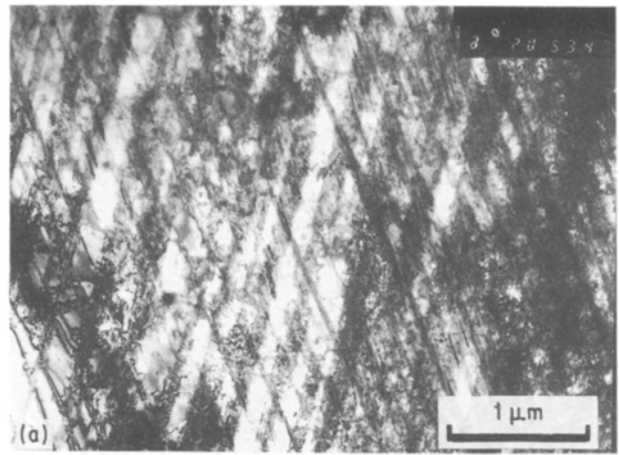


(d)

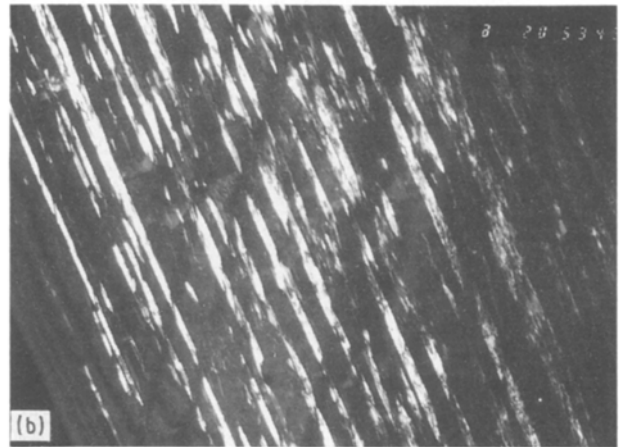
Figure 5 Percentage of twins as a function of their mean spacing in each family, for different calculated pressures corresponding to the observation depth ( $P_{\text{obs}}$ ): (a) No. 3 ( $P_{\text{obs}} = 15$  GPa), (b) No. 5 ( $P_{\text{obs}} = 17$  GPa), (c) No. 4 ( $P_{\text{obs}} = 22$  GPa), (d) No. 1 ( $P_{\text{obs}} = 31$  GPa).

previous foils and is estimated as about 58%.  $\alpha$  embryos were seen in 60% of the observed grains.

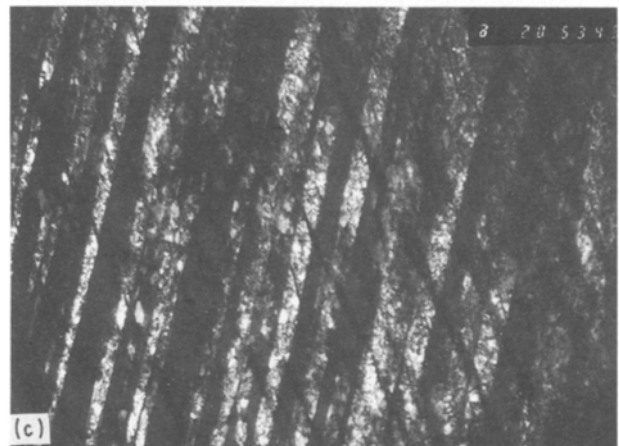
The fourth sample (test No. 1) was characterized by a laser energy of 70 J corresponding to a surface peak



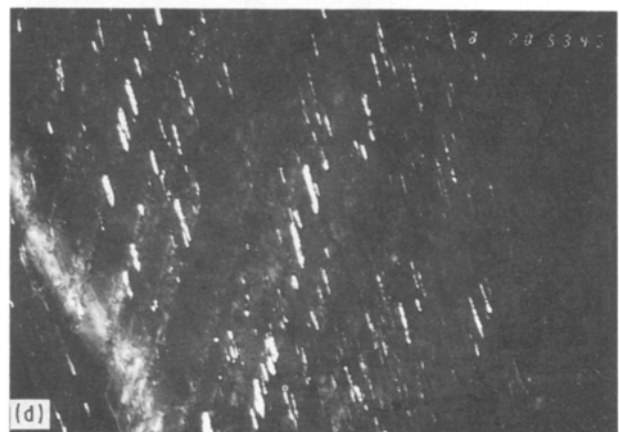
(a)



(b)



(c)



(d)

Figure 6 Transmission electron micrographs of sample 5 at a depth of 20  $\mu\text{m}$  corresponding to a 17 GPa shock pressure: (a) bright field showing two sets of twins in a (013) $\gamma$  section, (b) dark field showing one set of twins, (c) dark field showing a second set of twins which are in  $\epsilon$  phase (h.c.p. structure), (d) dark field showing  $\alpha$  embryos at the intersections of twin sets.

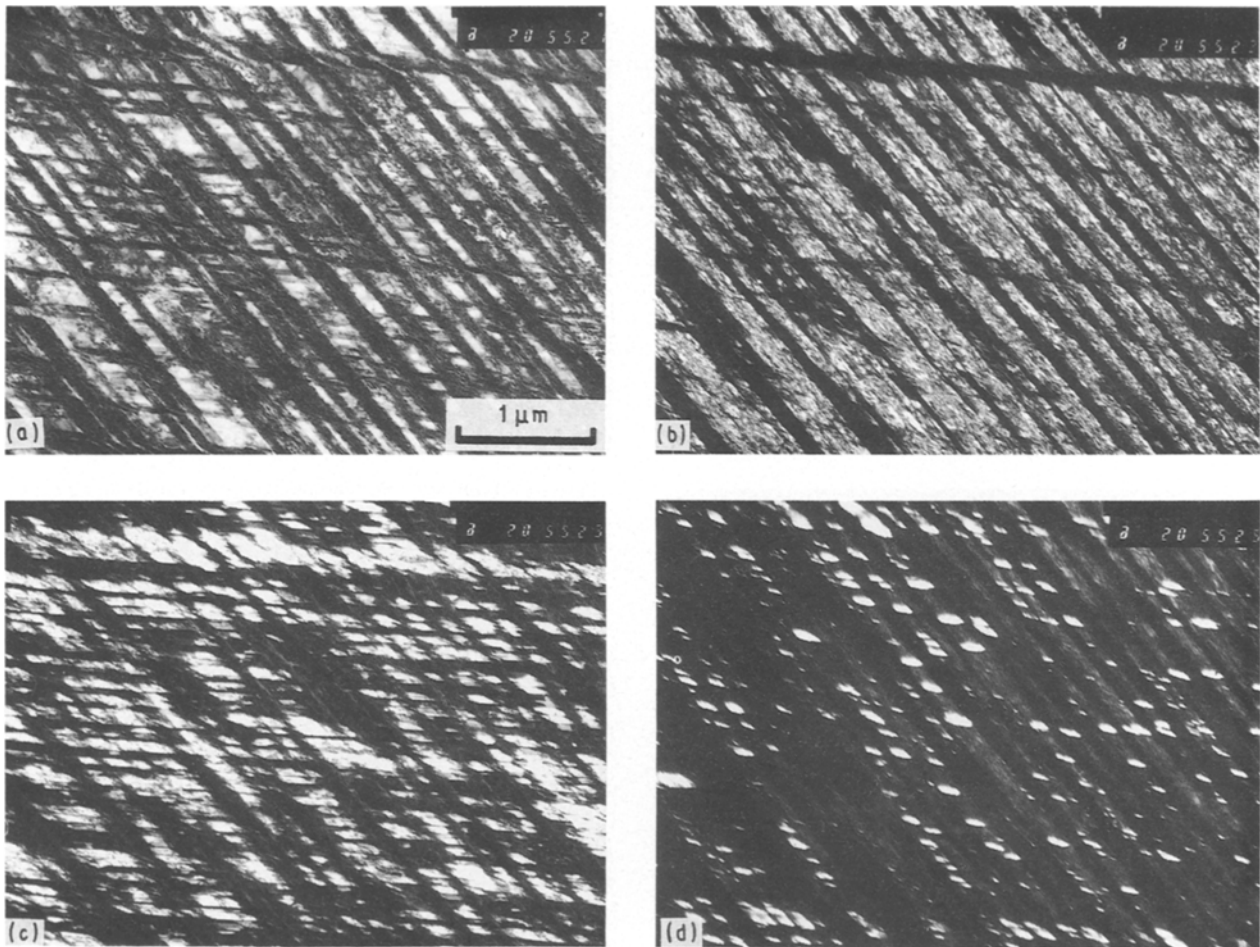


Figure 7 Transmission electron micrographs of sample 4 at a depth of 25  $\mu\text{m}$  corresponding to a 22 GPa shock pressure: (a) bright field showing two dense sets of twins in a  $(1\ 1\ 2)_\gamma$  section, (b) dark field showing one set of twins, (c) dark field showing a second set of twins, (d) dark field showing  $\alpha$  embryos at the intersections of twin sets.

pressure of 60 GPa but the observation depth being 30  $\mu\text{m}$ , the pressure at this depth is only 31 GPa which is nevertheless higher than in the previous samples. One could have thought that nearly the whole surface of the foil would be covered by three or four twin sets in each grain, but the areas occupied by respectively one or two twin sets are larger than in the foils with lower shock pressures (Fig. 4). Furthermore the shape of the twins is quite different; they appear very strongly fragmented (Fig. 8b) so that the bright fields are often very diffuse (Fig. 8a and c). Sometimes the twins are so dense and fragmented that it is quite impossible to distinguish between them and the matrix. The twin density is very high since the mean twin spacing of the whole sample is estimated to be 0.18  $\mu\text{m}$  and the percentage of twinned matter, although there are fewer areas with three or four twin sets than in the previous foils, is higher and reaches 61%. However no  $\alpha$  embryo was observed in this thin foil.

In the case of a low-pressure test (10 GPa, test No. 7), the microstructure is characterized by dislocation arrangements and very few twins (Fig. 9)

#### 4. Discussion

Microhardness measurements and observations performed by TEM confirm that the residual micro-

structure of the 304 stainless steel after a laser shock of very short pulse duration (0.6 ns) is nearly identical to the one obtained by a conventional shock, as we have already shown in the case of  $\alpha$ -Fe [6] and of the 304 and 316 stainless steels between 2.5 and 30 ns [7], in spite of pulse durations two or three orders shorter than for the conventional shocks. The microstructure evolution with pressure is particularly similar. A maximal effect of the shock wave on the samples is effectively observed between 25 and 50 GPa which is called the saturation range. In this pressure range, the surface microhardness reaches a maximum value and twinning is more frequent. For the pressure value of 31 GPa, although the number of twin sets is lower than after a shock of 22 GPa, the twin spacing is lower and finally the twinned matter is higher.

Inside the saturation range, the microhardness value at the treated surface is slightly lower after a laser shock than after a conventional shock; moreover the saturation range is more restricted. These two differences can be due either to a temperature effect because of insufficient thermal protection by the black paint, or to an effect of the pulse duration. However, the appearance threshold of the microhardness increase is similar and close to 8–10 GPa in the two cases of conventional and laser shocks.

For low values of pressure, the twin spacing is much more scattered (Fig. 5) than for higher pressures, as in



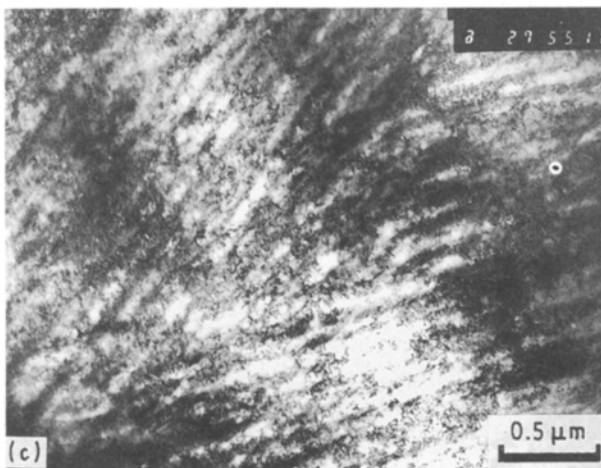
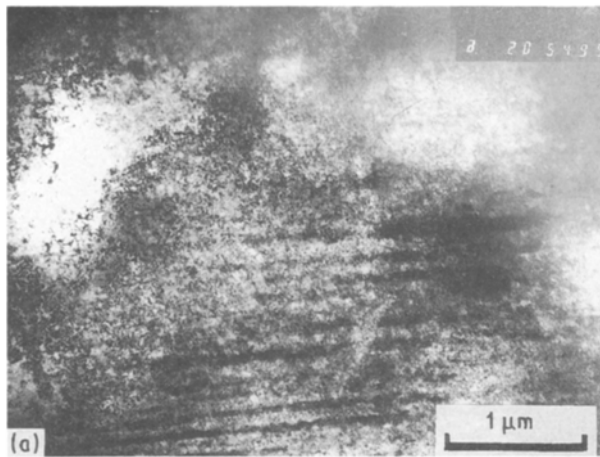


Figure 8 Transmission electron micrographs of sample 1 at a depth of 30  $\mu\text{m}$  corresponding to a 31 GPa shock pressure: (a) bright field showing two sets of twins in a  $(116)_{\gamma}$  section, (b) dark field showing the fragmented twins, (c) bright field showing two twin sets in another grain.

the case of conventional shocks [4]. For high values of pressure, as the number of twin sets decreases in every grain (Fig. 4), the number of twin intersections decreases; thus the number of favourable sites for  $\alpha$ -embryo formation decreases. However, as suggested by Staudhammer *et al.* [12], the temperature effect on  $\alpha$ -embryo formation is probably dominant. In our case, the disappearance of the  $\alpha$  phase at the highest pressure would thus be due more to the temperature rise induced by the shock (about 100 K for a 30 GPa

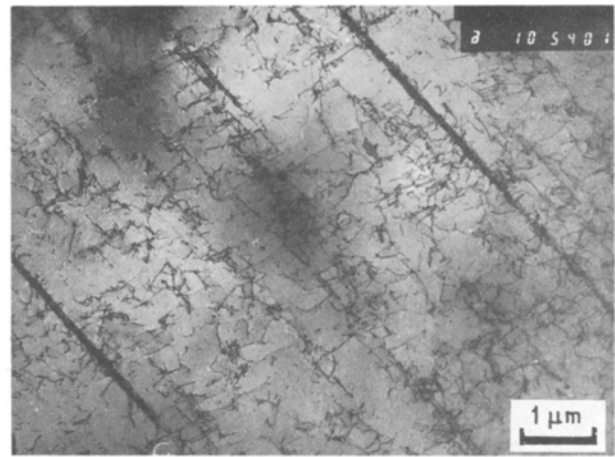


Figure 9 Transmission electron micrograph of sample 7 at a depth of 30  $\mu\text{m}$  corresponding to a 10 GPa shock pressure.

shock pressure [13]) than to a decrease of the potential number of sites. The difficulty of putting into contrast in bright field or in dark field all the  $\alpha$ -phase embryos and their small size have not allowed us to calculate the  $\alpha$ -phase percentage in the samples. Only the percentage of grains where  $\alpha$  phase occurs was determined. However, it is clear that the size of the  $\alpha$  embryos formed with a 0.6 ns pulse duration by a laser shock is slightly smaller than the size of the  $\alpha$  embryos formed by a conventional shock with a pulse duration of the order of 1  $\mu\text{s}$  [3], but the 0.6 ns embryo thickness is much higher than the minimum thickness proposed by Staudhammer *et al.* [12].

## 5. Conclusion

The effect of pressure on the microstructure of a 304 stainless steel submitted to shock waves generated by a 0.6 ns pulsed laser was studied. The results are summarized as follows:

1. The effects induced by laser shock are very similar to those produced by conventional shock, in spite of a much shorter pulse duration.
2. Microhardness increases with peak pressure up to 25 GPa (corresponding to a laser intensity of  $0.5 \times 10^{12} \text{ W cm}^{-2}$ ), then remains rather constant up to 55 GPa (laser intensity  $1.5 \text{ W cm}^{-2}$ ), then decreases at higher peak pressures.
3. The number of twin sets increases with pressure up to 25 GPa, then decreases, but the mean twin spacing continuously decreases.
4.  $\alpha$ -phase embryos are observed within the pressure range 15–25 GPa.

## References

1. L. E. MURR and M. F. ROSE, *Phil. Mag.* **18** (1968) 281.
2. K. P. STAUDHAMMER, C. E. FRANTZ, S. S. HECKER and L. E. MURR, in "Shock Waves and High Strain-Rate Phenomena in Metals: Concepts and Applications", edited by M. A. Meyers and L. E. Murr (Plenum, New York, 1981) p. 91.
3. L. E. MURR and K. P. STAUDHAMMER, *Mater. Sci. Engng* **20** (1975) 35.

4. L. E. MURR, in "Shock Waves and High Strain-Rate Phenomena in Metals : Concepts and Applications", edited by M. A. Meyers and L. E. Murr (Plenum, New York, 1981) p. 607.
5. A. R. CHAMPION and R. W. ROHDE, *J. Appl. Phys.* **41** (1970) 2213.
6. M. HALLOUIN, M. GERLAND, J. P. ROMAIN, F. COTTET and L. MARTY, *J. Physique, Coll. C3, Suppl.* No. 9 (1988) 413.
7. M. HALLOUIN and M. GERLAND, *Mém. Etudes Sci. Rev. Métall.* **9** (1989) 506.
8. R. FABBRO, E. FABRE, F. AMIRANOFF, C. GARBAN-LABAUME, J. VIRMONT, M. WEINFELD and C. E. MAX, *Phys. Rev. A* **26** (1982) 2289.
9. J. GRUN, R. DECOSTE, B. H. RIPIN and J. GARDNER, *Appl. Phys. Lett.* **39** (1981) 545.
10. F. COTTET and M. BOUSTIE, *J. Appl. Phys.* **66** (1989) 4067.
11. H. BUCKLE, Publications scientifiques et techniques du ministère de l'air N T 90 (Paris, 1960).
12. K. P. STAUDHAMMER, L. E. MURR and S. S. HECKER, *Acta Metall.* **31** (1983) 267.
13. R. G. McQUEEN, S. P. MARSH, J. W. TAYLOR, J. N. FRITZ and W. J. CARTER, in "High Velocity Impact Phenomena", edited by R. Kinslow (Academic, New York, 1970) p. 293.

*Received 16 July 1991  
and accepted 17 February 1992*